Denaturation of hen egg white lysozyme in electromagnetic fields: a molecular dynamics study

N. English* and D. Mooney

School of Chemical and Bioprocess Engineering, The Centre for Synthesis and Chemical Biology, Conway Institute of Biomolecular and Biomedical Research, University College Dublin, Belfield, Dublin 4, Ireland. *niall.english@ucd.ie

ABSTRACT

Nonequilibrium molecular dynamics simulations of hen egg white lysozyme have been performed in the canonical ensemble at 298 K in the presence of external electromagnetic fields of varying intensity in the microwave to far-infrared frequency range. Significant non-thermal field effects were noted, such as marked changes in the protein's secondary structure which led to accelerated incipient local denaturation relative to zero-field conditions. This occurred primarily as a consequence of alignment of the protein's total dipole moment with the external field. The applied field intensity was found to be highly influential on the extent of denaturation in the frequency range studied, and 0.25-0.5 $VÅ^{-1}_{rms}$ fields were found to induce initial denaturation to a comparable extent to thermal denaturation in the 400 to 500 K range. In subsequent zero-field simulations following exposure to the e/m field, the extent of perturbation from the native fold and the degree of residual dipolar alignment were found to be influential on incipient folding.

Keywords: electromagnetic field, molecular dynamics, protein, water, hydrogen bonding

1 INTRODUCTION

The thermal effects of electromagnetic (e/m) fields on macromolecules stem from heat generation by e/m energy absorption. However, the precise mode of action for non-thermal e/m field effects remains unknown [1,2], although it is thought that fields excite macromolecule vibrational modes, altering conformations. The effects of non-thermal modes are surprising, *e.g.* reversible changes in protein activity [3]. The question of non-thermal effects on protein stability, and hence function, in far IR and microwave fields has been the subject of extensive debate, *e.g.* in relation to mobile communication signals on human health [4]. Owing in part to health problems of exposure to e/m fields [5], there exists a body of experimental work on e/m effects on protein denaturation and stability [6-8]. On a wider level, however, a strong motivation for the study of e/m field effects on proteins lies in the possibility of influencing alterations in protein structure by e/m fields of well-defined frequency and intensity. This would open up a wide range of possibilities in protein engineering and medicine [9-10].

In recent years, computer simulation has contributed greatly to molecular-level understanding of protein function and folding [11]. To complement experimental studies of e/m field effects [1-3,6-8], it would be of interest to use molecular simulation to model field effects on proteins. Recent molecular dynamics (MD) simulations have studied both thermal and non-thermal effects of microwave and far IR fields on water [12-14], hydrates [15], metal oxides [16], zeolites [17] and polystyrene solutions [18]. This work is concerned with MD studies of non-thermal field effects on heg egg white lysozyme (HEWL). HEWL was chosen because of its use in previous MD studies [19-21] and its extensive experimental scrutiny. This protein of 129 residues contains two structural domains, denoted α and β, and is stabilized by four disulfide bridges [22]. The α-domain contains four α-helices and a 3_{10} helix while the β-domain consists of a triple-stranded anti-parallel β-sheet, a long loop and a 3_{10} helix.

2 METHODOLOGY

The simulations were performed using the CHARMM 27 [23] and TIP3P [24] potentials for HEWL and water, respectively; CHARMM potentials were parameterized with TIP3P. The crystal structure of triclinic HEWL [22], an oxidized form with the four disulfide bridges intact, served as the starting structure. Formal charges were chosen appropriate to pH 7, giving in a total protein charge of +8*e*, and hydrogen atoms were added. The protein was placed at the center of a rectangular periodic box with (*x*,*y*,*z*) dimensions of 50, 55.5 and 62 Å, respectively, to which 5,124 water molecules were added, resulting in a system of 17,332 atoms. van der Waals interactions were treated using a twin-range method [25], with cut-off radii of 12 and 15 Å, respectively. The reaction field method [26] was used for long-range electrostatics, with a cut-off radius of 15 Å. The dielectric constant in this technique was optimized to minimize the RMS error in electrostatic forces with respect to the 'definitive' Lekner method [27] for a relaxed system at 298 K [16]. The system size was deemed sufficient by comparison of protein-water interaction energies for relaxed configurations with those of two larger systems. The MD time step was 1 fs and a 1 ps period was used for the NVT thermal reservoir. The system was 'heated' to 298 K in 20 K increments in 5 ps steps, and was then relaxed for a further 0.25 ns at 298 K.

Uniform e/m fields were applied with the electric and magnetic components **E** and **B** in the *z*- and *y*- directions, *i.e.* $\mathbf{E}(t) = E_{max}\cos(\omega t)\mathbf{k}$ and $\mathbf{B}(t) = B_{max}\cos(\omega t)\mathbf{j}$ [12,13]

$$m_i\ddot{\mathbf{r}}_i = \mathbf{f}_i + q_i\mathbf{E}(t) + q_i\mathbf{v}_i \times \mathbf{B}(t) \qquad (1)$$

where q_i denotes the charge and $\mathbf{f}_i$ the force on site i due to the potential. Classical mechanics was considered valid to model e/m absorption, since the experimental spectrum of liquid water is continuous [28,29]. The fields were of frequency ν = 50 to 500 GHz (1.67 to 16.7 cm^{-1}) and of RMS intensity E_{rms} = 0.1 to 0.5 V/Å. From equilibrium zero-field simulations, the electric field intensities in condensed water phases are in the 1.5 to 2.5 V/Å range [13]. The field intensity applied in this study is several orders of magnitude larger than those applied typically, either experimentally or industrially [9]. However, previous MD simulations of e/m fields on water [12-14] and other materials [15-18] have shown it is necessary to use field intensities of the order of 0.1 V/Å to observe tangible effects within the limited timescales amenable to simulation. The fields were applied in the NVT ensemble to isolate field effects from thermal effects, and are referred to as non-equilibrium NVT (NNVT) simulations.

A series of NNVT simulations were carried out at 298 K for 0.5 ns in fields of frequency 50, 100, 200 and 500 GHz with RMS intensities of 0.1, 0.15 0.25 and 0.5 V/Å, using the relaxed system as a starting configuration. This was of sufficient duration to investigate initial field-induced denaturation of the protein, rather than to determine full unfolding pathways. A reasonable number of cycles of the field can also be applied in this time (with a maximum period of 20 ps for the 50 GHz field). To assess the reversibility of denaturation, subsequent zero-field NVT simulations were performed after many of the NNVT simulations for at least 1 ns.

3 RESULTS AND DISCUSSION

Marked changes in the protein secondary structure were observed during the NNVT simulations vis-à-vis a parallel zero-field NVT simulation for 0.5 ns (*i.e.* beyond the initial 0.25 ns relaxation), which led to accelerated incipient denaturation. Below 0.25 $VÅ^{-1}_{rms}$ intensity, non-thermal field effects were found to be more limited. Fig. 1 depicts a representation of the DSSP-determined secondary structure [30] at various stages for a typical example of denaturation behavior in a 100 GHz / 0.5 $VÅ^{-1}_{rms}$ field. There is a more rapid loss of the triple-stranded β-sheet and 3_{10} helix structures in the β-domain, occurring within less than 0.1 ns, while the α-helices in the α-domain are somewhat more persistent, in particular the C α-helix. Visual inspection of the DSSP secondary structure showed the β-domain tended to lose its salient features more rapidly in all simulations with E_{rms} of 0.25 V/Å or greater, in contrast to zero-field simulation where the prominent features of both domains were largely preserved for the 0.5 ns trajectory. However, some parts of the α-domain were found to be highly mobile in response to external fields, in particular solvent-exposed terminal loop regions such as Lys1-Val2-Phe3.

To investigate the incipient denaturation further, the all-atom and α-carbon root mean square deviation (RMSD) of HEWL relative to its crystal structure was determined, in addition to the RMSD's of each domain. The mean protein radius and α-β inter-domain distance were also calculated (between their respective centers of mass). As a representative example of behavior in fields of E_{rms} of 0.25 V/Å or greater, the all-atom and α-carbon RMSD's for the whole protein are shown in Fig. 2 in 0.5 $VÅ^{-1}_{rms}$ fields for 50 to 200 GHz. For comparison with zero-field partial thermal denaturation, all-atom RMSD's are shown at 400 and 500 K, after the 0.25 ns period of relaxation at 298 K. Under zero-field conditions at 298 K, the all-atom and α-carbon RMSDs reach plateaux vis-à-vis the crystal structure

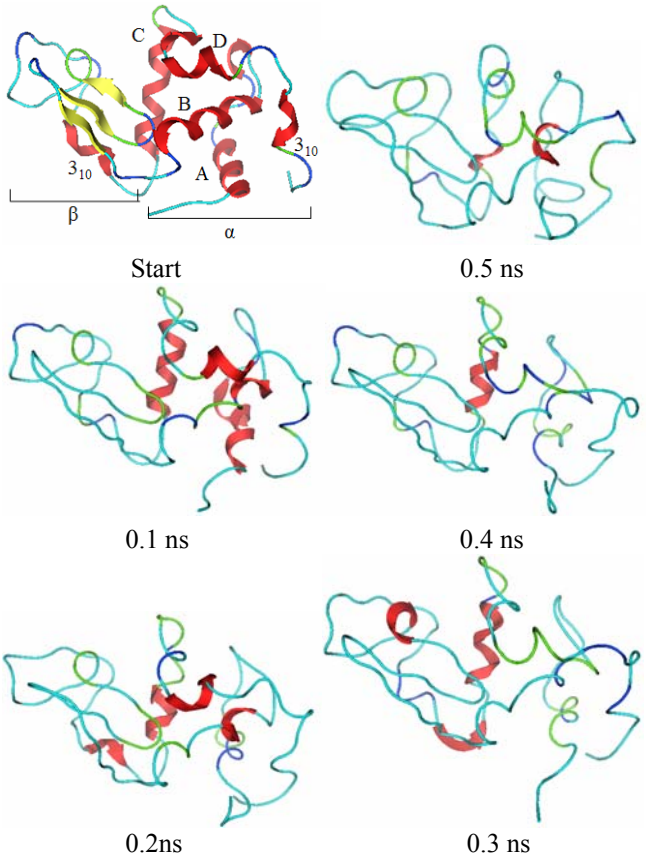

Figure 1: Schematic representation of HEWL fold at various stages in a 100 GHz / 0.5 $VÅ^{-1}_{rms}$ field at 298 K. The ribbon structures have been drawn according to DSSP secondary structure assignment [30]. There are two domains, with the α-domain represented on the right and the β-domain on the left. In the native fold, the α-domain consists of four α-helices A, B, C, D (residues 4-15, 24-36, 89-99 and 108-115, respectively) and a 3_{10} helix (residues 120-124), while the β-domain contains a triple-stranded anti-parallel β-sheet (41-45, 50-53 and 58-60), a long loop (61-78) and a 3_{10} helix (80-84). The overall structure is stabilized by four disulfide bridges.

after around 0.2 ns, and increase little beyond the respective values of around 2.1 and 1.6 Å in the initial relaxed structure. Upon the application of external fields, however, there is a dramatic increase in both the all-atom and α-carbon RMSD values within the first 0.1 ns as the system adjusts to the field, to about 2.5 times that under zero-field conditions, with a greater slope thereafter. The fact that this behavior is observed to a more limited extent in the α-carbon case demonstrates that backbone motion is influenced to a certain degree by the applied field, in addition to sidechain movement. The larger slope of the RMSD curves beyond the first 0.1 ns transient of field application indicates a substantial enhancement of atomic mobility in comparison to the zero-field case, via the Einstein relation [13-16]. In the initial period of adjustment to the applied field, it was found that the promotion in RMSD for the whole protein was attributable primarily to a rise in inter-domain separation, after which the individual domains tended to expand. Domain all-atom and α-carbon RMSD curves indicated that the β-domain experienced a greater extent of perturbation by the applied field (not shown here), which is consistent with the visual observation of DSSP secondary structure. It was found that 100 GHz (corresponding to a field period of 10 ps) tends to increase the RMSD to the greatest extent for a given intensity. This is consistent with observations of e/m field-enhanced molecular mobility for liquid water at 298 K using a variety of potentials, due to dipolar alignment with the external field [13-16]. The observation of localized aspects of denaturation in e/m fields in highly solvent-exposed regions, e.g. for the terminal loop Lys1-Val2-Phe3, suggests that the dipolar alignment and mobility of water molecules are influential on this process in these regions.

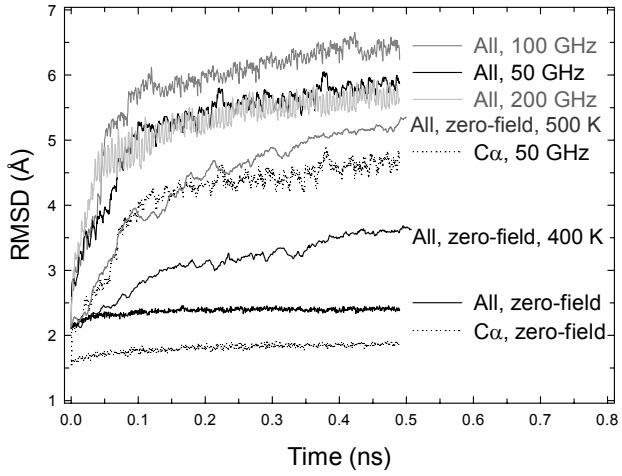

Figure 2: All-atom and α-carbon root mean square deviation of HEWL vis-à-vis the crystal structure at 298 K in 0.5 $VÅ^{-1}_{rms}$ fields and at zero-field conditions, after 0.25 ns of zero-field equilibration. The frequency or conditions are indicated on the right of each curve. Zero-field all-atom RMSD curves are also shown at 400 and 500 K.

During partial themal denaturation at 400 and 500 K, the RMSD curves increased rapidly within the first 0.15 ns to approximately 1.25 and 1.75 times that of the zero-field RMSD at 298 K, with similar slopes to the 0.5 $VÅ^{-1}_{rms}$ cases at 50 to 200 GHz thereafter. However, the increase in the inter-domain separation was not as marked in this period as that observed in the shorter 0.1 ps transient for the 0.5 $VÅ^{-1}_{rms}$ fields. Within the 50 to 200 GHz range, it was found that e/m field intensity plays an important role in determining the extent of denaturation. For instance, a 100 GHz / 0.5 $VÅ^{-1}_{rms}$ field induced shifts in secondary structure to a greater and more rapid degree than thermal denaturation at 500 K: the RMSD was found to be some 30 to 40% larger, with a transient of 0.1 versus 0.15 ps (cf. Fig. 2). In contrast, the 0.25 $VÅ^{-1}_{rms}$ fields were found to result in less dramatic and more gradual increases in RMSD: for example, the 100 GHz / 0.25 $VÅ^{-1}_{rms}$ field led to an RMSD evolution of around 10 % lower than the 400 K thermal denaturation case (not shown in Fig. 2 for clarity).

In Fig. 3, the ratio is presented of the averaged total protein *z*-dipole alignment with various external fields, *i.e.* at the **E** maxima in *z*+ and *z*- directions, $\langle M_{z+} - M_{z-} \rangle$, to the average magnitude of the total protein dipole moment under zero-field conditions, $\langle |\mathbf{M}| \rangle_0$. 50 to 100 GHz is the most effective frequency range for maximal protein dipole response, although the alignment of water molecule dipoles is also important in this range [13,14]. It appears that the protein dipolar alignment determines the degree of partial denaturation, as characterized by the RMSD curves in Fig. 2, in which the 100 GHz field tends to maximize the degree of incipient denaturation. From Fig. 3, for a field intensity below 0.25 $VÅ^{-1}_{rms}$ the protein dipolar response is weaker, and denaturation was found to be significantly more limited. It has been established by English *et al*. [13,14] that water molecules' dipoles align significantly with fields in the 0.1 and 0.2 $VÅ^{-1}_{rms}$ intensity range between 50 and 100 GHz, and that molecular mobility is enhanced substantially, from observations of the mean square displacement via the Einstein relation. This indicates that it is primarily the breakage of key stabilizing intra-protein hydrogen bonds which leads to the observed partial denaturation at field intensities of 0.25 $VÅ^{-1}_{rms}$ or greater. However, the ready alignment and enhanced mobility of water molecules at these field intensities can also be expected to be influential, especially on motion of more solvent-exposed sidechains.

After field exposure, subsequent zero-field simulations with durations of the order of a nanosecond demonstrated that neither the evolution of the RMSD for the all-atom case nor that for α-carbons (relative to the crystal structure) began to level off or reduce to the level prior to application of the 0.25 / 0.5 $VÅ^{-1}_{rms}$ fields; rather, the RMSD continued to increase. However, below an intensity of 0.25 $VÅ^{-1}_{rms}$, there was little increase in RMSD after termination of the field application. Several system configurations with differing all-atom protein RMSDs vis-à-vis the crystal structure (2.5 to 6 Å) were taken from the 100 GHz / 0.5 $VÅ^{-1}_{rms}$ run to assess the perturbation in secondary structure

NSTI-Nanotech 2007, www.nsti.org, ISBN 1420061828 Vol. 1, 2007

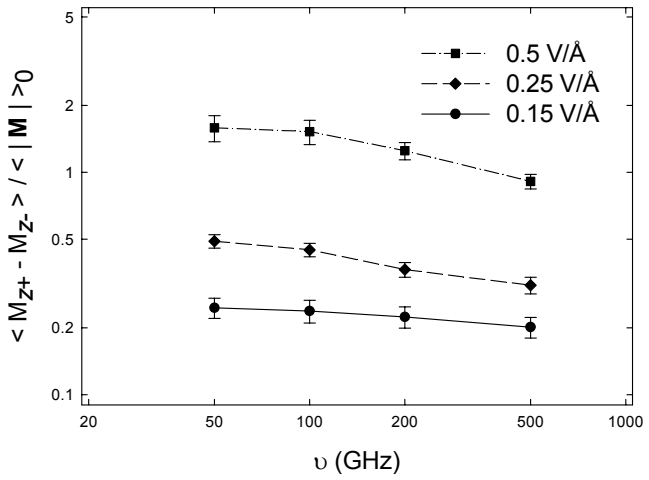

Figure 3: Ratio of the averaged HEWL *z*-dipole alignment at 298 K, $<M_{z+} - M_{z-}>$, in various external fields to the average magnitude of the total protein dipole moment under zero-field conditions, $<|\mathbf{M}|>_0$.

upon the reversibility of field-induced denaturation. It was generally found that the lower the RMSD, the lower the extent of its increase in subsequent simulations. However, the dipolar orientation of the protein and water at the instant of field deactivation was also found to be influential on subsequent initial 'folding': for near-zero degrees of dipole alignment, *i.e.* after a lag time for the 10 ps field cycle at which $\mathbf{E}(t) = E_{max}\cos(\omega t)\mathbf{k}$ leads to $\mathbf{E}(t) = 0\mathbf{k}$, the increase in RMSD was at a minimum; randomization of orientation from a more aligned state appears to retard initial folding.

4 CONCLUSIONS

Significant non-thermal field effects were noted in NNVT simulations, such as marked changes in HEWL secondary structure which led to localized preliminary denaturation. This observation is significant, in view of health concerns related to exposure to e/m fields [5] and possible experimental findings of non-thermal field effects on biological systems [1-3,6-8]. Denaturation occurred primarily as a consequence of alignment of the protein's total dipole moment with the external field and is consistent with intra-protein hydrogen bond breakage.

Although this preliminary study is concerned with incipient field-induced denaturation, rather than complete unfolding pathways, some insights into the initial stages of folding and unfolding may be obtained. The field intensity was found to be very influential on the extent and speed of onset of denaturation, and 0.5 $VÅ^{-1}_{rms}$ fields led to more extensive denaturation than preliminary thermal unfolding at 500 K over the same period. The secondary structure perturbation affects incipient folding, as does the dipolar alignment at the instant of field deactivation. These observations, together with limitations of accuracy of the current generation of fixed charge protein force fields and the necessarily short-time scales, raise interesting questions on the reversibility of field-induced denaturation.

REFERENCES

[1] D. de Pomerai, B. Smith, A. Dawe, K. North, T. Smith, D. Archer, I. Duce, D. Jones & P. Candido, FEBS Letters 543, 93, 2003.
[2] M. Porcelli, G. Cicciapuoti, S. Fusco & R. Massa, FEBS Letters 402, 102, 1997.
[3] L. Taylor, Bioelectromagnetics 2, 259, 1995.
[4] M. Repacholi, Tox. Letters 120, 323, 2001.
[5] L. Challis, Bioelectromagnetics 26, S98, 2005.
[6] H. Bohr & J. Bohr, Phys. Rev. E 61, 4310, 2000.
[7] R. Weissenborn, K. Diederichs, W. Welte, G. Maret & T. Gisler, Acta Crystallographica D 61, 163, 2005.
[8] B. Réjasse, T. BessonEn, M. Legoy & S. Lamare, Org. Biomol. Chem. 4, 3703, 2006.
[9] J. Thuéry, "Microwaves: Industrial, Scientific and Medical Applications", Artech, 1992.
[10] A. Phelan, C. Neubauer, R. Timm, J. Neirenberg & D. Lange, Radiat. Res. 137, 52, 1994.
[11] C. Dobson, A. Šali & M. Karplus, Angew. Chem. Int. Ed. 37, 868, 1998.
[12] N. English & J. MacElroy, J. Chem. Phys. 118, 1589, 2003.
[13] N. English & J. MacElroy, J. Chem. Phys. 119, 11806, 2003.
[14] N. English, Molec. Phys. 104, 243, 2006.
[15] N. English & J. MacElroy, J. Chem. Phys. 120, 10247, 2004.
[16] N. English, D.C. Sorescu & J. Johnson, J. Phys. Chem. Solids 67, 1399, 2006.
[17] C. Blanco & S. Auerbach, J. Phys. Chem. B 107, 2490, 2003.
[18] M. Purdue, J. MacElroy, D. O'Shea, M. Okuom & F. Blum, J. Chem. Phys. 124, 204904, 2006.
[19] P. Hünenberger, A. Mark & W. van Gunsteren, Proteins 21, 196, 1995.
[20] L. Smith, A. Mark, C. Dobson & W. van Gunsteren, J. Mol. Biol. 280, 703, 1998.
[21] B. Gilquin, C. Guilbert & D. Perahia, Proteins 41, 58, 2000.
[22] M. Ramanadham, L. Sieker, & L. Jensen, Acta Crystallo. A (Suppl.) 43, 13, 1987.
[23] A. MacKerell Jr., M Feig & C. Brooks III, J. Comput. Chem. 25, 1400, 2004.
[24] W. Jorgensen, J. Chandrasekhar, J. Madura, R. Impey & M. Klein, J. Chem. Phys., 79, 926, 1983.
[25] W. van Gunsteren & H. Berendsen, Angew. Chem. Int. Ed. Engl. 29, 992, 1990.
[26] M. Neumann, J. Chem. Phys. 82, 5663, 1985.
[27] J. Lekner, Physica A 157, 826, 1989; J. Lekner, Physica A 176, 485, 1991.
[28] M. Asfar & J. Hasted, J. Opt. Soc. Am. 67, 902, 1977.
[29] H. Zelsmann, J. Mol. Struct. 350, 95, 1995.
[30] W. Kabsch & C. Sander, Biopolymers 22, 2577, 1983.